

Structural, Electronic, and Optical Properties of Representative Cu–Flavonoid Complexes

Ch. E. Lekka,^{*,†} Jun Ren,[‡] Sheng Meng,[‡] and Efthimios Kaxiras^{‡,§,||}

Department of Materials Science and Engineering, University of Ioannina, Ioannina 45110, Greece, and Department of Physics, School of Engineering and Applied Sciences, and Department of Chemistry and Chemical Biology, Harvard University, Cambridge, Massachusetts 02138

Received: September 8, 2008; Revised Manuscript Received: January 28, 2009

We present density functional theory (DFT) results on the structural, electronic, and optical properties of Cu–flavonoid complexes for molar ratios 1:1, 1:2, and 1:3. We find that the preferred chelating site is close to the 4-oxo group and in particular the 3–4 site followed by the 3'–4' dihydroxy group in ring B. For the Cu–quercetin complexes, the large bathochromic shift of the first absorbance band upon complexation, which is in good agreement with experimental UV–vis spectra, results from the reduction of the electronic energy gap. The HOMO states for these complexes are characterized by π -bonding between the Cu d orbitals and the C, O p orbitals except for the case of 1:1 complex (spin minority), which corresponds to σ -type bonds. The LUMO states are attributed to the contribution of Cu p_z orbitals. Consequently, the main features of the first optical absorption maxima are essentially due to $\pi \rightarrow \pi^*$ transitions, while the 1:1 complex exhibits also $\sigma \rightarrow \pi^*$ transitions. Our optical absorption calculations based on time-dependent DFT demonstrate that the 1:1 complex is responsible for the spectroscopic features at pH 5.5, whereas the 1:2 complex is mainly the one responsible for the characteristic spectra at pH 7.4. These theoretical predictions explain in detail the behavior of the optical absorption for the Cu–flavonoid complexes observed in experiments and are thus useful in elucidating the complexation mechanism and antioxidant activity of flavonoids.

I. Introduction

Flavonoids have broad pharmacological uses due to their antibacterial, antiosteoporotic, and anticancer actions, which derive from their effective interaction with several enzymes.^{1–3} In addition, flavonoids exhibit antioxidant activity, that is, they prevent the damage of biomolecules by free radicals and reduce the effects of such damage, which is responsible for several diseases and aging.^{4,5} The antioxidant activity of flavonoids is related to chelation of metal ions, which catalyze the production of hydroxyl and lipid radicals through the decomposition of preformed lipid hydroperoxides.^{6,7} In particular, iron and copper ions play a major role in the production of the very reactive hydroxyl radical (HO \cdot) through the Fenton and Haber–Weiss reactions.^{8–11} Chelation of these ions with flavonoids may be a natural way to reduce or eliminate their undesirable catalytic behavior; in fact, metal–flavonoid complexes may be a preferred way of ion chelation as compared to synthetic chelators that can exhibit toxicity problems.¹²

The antioxidant activity of flavonoids and metal–flavonoid complexes has been the subject of numerous studies,^{8–11,13–23} and several attempts have been made to elucidate the structure–activity relationship.^{8–12,20–23} These studies have shown that the ability of flavonoids to bind metals (such as Fe, Cu, Al, Zn, Ga, and In) is related to the presence of certain key structural features: (i) the *ortho*-dihydroxyl structure in either ring A or B and (ii) the hydroxyl moiety at position 3 in combination with the oxo-group at position 4 of ring C. Much attention has been paid to Fe ions, the most abundant type of

metal ion in living organisms. Our recent theoretical study demonstrated convincingly the optimal chelation site of Fe ions with flavonoids and examined the resulting electronic and optical properties.²⁴ There is much less theoretical understanding of the complexation mechanism of flavonoids with Cu ions, an essential trace element in living systems. In the case of Cu ions, some studies of electrospray ionization mass spectrometry⁹ showed the formation of different metal-to-flavonoid molar ratios, depending on the pH value, which is an intriguing observation with potentially important clues into the complexation mechanism. The 1:1 and 1:2 metal–flavonoid complexes at pH ≤ 5 result in a large bathochromic shift for the first absorption peak, whereas the 1:3 complex has been suggested to correspond to the absorption at pH 7.4. The origin of the different optical absorption spectra of the 1:1, 1:2, and 1:3 complexes and their corresponding relationship with the electronic properties remains unclear.

The aim of the present work is to investigate the complexation of Cu ions with some representative flavonoids, using first-principles calculations based on density functional theory (DFT). In addition, we calculate the ultraviolet–visible (UV–vis) spectra for the different Cu–quercetin complexes, using time-dependent DFT (TDDFT), and compare these spectra to experimental results.

This article is organized as follows. The computational methods we used are discussed in section II. We present our results of the optimal structure for the Cu–flavonoids complexes in section III. Section IV discusses the calculated electronic properties and optical absorption spectra. Finally, a summary of our results is given in section V.

II. Computational Methods

We performed standard Kohn–Sham self-consistent DFT calculations using the local density approximation (LDA) with

* To whom correspondence should be addressed. Telephone: +302651097310. Fax: +302651097037. E-mail: chlekka@cc.uoi.gr.

[†] University of Ioannina.

[‡] Department of Physics, Harvard University.

[§] School of Engineering and Applied Sciences, Harvard University.

^{||} Department of Chemistry and Chemical Biology, Harvard University.

TABLE 1: Energies and Structural Parameters for Different Cu–Flavonoid Complexes^a

complex	site	E_b (eV)	E_b' (eV)	N	d (Å)
Cu–Que	3–4	2.43	2.26	2	1.97
	4–5	1.65	1.49	2	1.87
	$3_{H'}-4'$	1.53	0.85	1	1.87
	$3'-4'$	1.18	0.78	2	1.93
Cu–2Que	(3–4;3–4) ^c	2.27	1.95	4	1.95
	(3–4;3–4) ^a	2.05	1.73	4	1.96
	(3–4;3–4) ^b	2.02	1.70	4	1.94
	(4–5;4–5) ^a	1.71	1.38	4	1.93
	(4–5;4–5) ^b	1.80	1.48	4	1.89
	(3–4;4–5) ^a	1.95	1.63	4	1.92
Cu–3Que	(3–4;3–4;3–4)	1.00	0.52	6	1.98
	(3–4;3–4;4–5)	0.74	0.26	6	1.99
	(3–4;4–5;4–5)	0.50	0.02	6	1.97
	(4–5;4–5;4–5)	0.14	0.34	6	1.99
Cu–Lut	4–5	1.78	1.62	2	1.84
	$3_{H'}-4'$	0.96	0.80	1	1.80
	$3'-4'$	0.56	0.23	2	1.93
Cu–2Lut	(4–5;4–5) ^a	2.03	1.70	4	1.92
	(4–5;4–5) ^b	2.05	1.73	4	1.90
Cu–3Lut	(4–5;4–5;4–5)	0.29	0.20	6	2.04
Cu–Gal	3–4	2.26	2.10	2	2.00
	4–5	2.21	2.05	2	2.01
Cu–2Gal	(3–4;3–4) ^c	2.35	2.02	4	1.96
	(3–4;3–4) ^a	2.25	1.93	4	1.91
	(3–4;3–4) ^b	2.23	1.90	4	1.92
	(4–5;4–5) ^a	1.89	1.60	4	1.89
	(4–5;4–5) ^b	1.96	1.64	4	1.89
	(3–4;4–5) ^a	2.14	1.82	4	1.91
Cu–3Gal	(3–4;4–5) ^b	2.06	1.74	4	1.91
	(3–4;3–4;3–4)	1.16	0.67	6	2.04
	(3–4;3–4;4–5)	1.03	0.55	6	2.05
	(3–4;4–5;4–5)	1.14	0.66	6	2.00
	(4–5;4–5;4–5)	0.27	0.21	6	1.96

^a The Cu binding energy (E_b and E_b') with respect to different reservoir choice for the removed H atoms, number of Cu–O bonds (N), and average Cu–O bond length (d) are listed. H atoms are removed from the OH sites where Cu binds, unless the site is denoted with a subscript H, in which case the H atom of the OH unit at that site is still present after the Cu ion has been attached.

the SIESTA code.^{25–27} Core electrons were replaced by norm-conserving pseudopotentials²⁸ in the fully nonlocal Kleinman–Bylander form,²⁹ and the basis set is a general and flexible linear combination of numerical atomic orbitals (NAOs) constructed from the eigenstates of the atomic pseudopotentials.³⁰ The NAOs are confined, being strictly zero beyond a certain radius. For every C atom the basis set includes 13 NAOs: two radial shapes to represent the 2s states with confinement radii $r_s = 5.12$ au, and two additional 2p shells plus a polarization p shell with confinement radii $r_p = r_p^{\text{Pol}} = 6.25$ au. For every H atom we have five NAOs: two radial shapes for the 1s orbital and a polarization s orbital with confinement radii $r_s = r_s^{\text{Pol}} = 6.05$ au. For every O atom we have 13 NAOs: two 2s shells, two 2p shells, and a p polarization shell with confinement radii $r_s = 3.93$ au and $r_p = r_p^{\text{Pol}} = 4.93$ au, respectively. Finally, for the Cu atom we use 25 NAOs: two 4s shells, two 4p shells, two 3d shells, and a p polarization shell with confinement radii $r_s = 8.03$ au, $r_p = 12.27$ au, and $r_d = r_d^{\text{Pol}} = 4.75$ au, respectively. The performance of the double- ζ polarized orbitals basis set made of NAOs has been tested for a variety of systems³⁰ and found to give quantitative results for structural, electronic, and optical properties of biological molecules.^{24,32,33} Especially in our case, since the Cu–quercetin (Que) binding has covalent character, the basis-set superposition is very small (~ 10 meV) and neglected, as compared to the bonding energies (~ 1 eV) reported in Table 1. For the exchange-correlation functional, we used the Ceperley–Alder form (as parametrized by Perdew and Zunger) of the LDA and we constructed our pseudopotentials

within the same approximation. Finally, an auxiliary real space grid equivalent to a plane-wave cutoff of 100 Ry is used.

As representative examples for the flavonoid classes, we chose luteolin (Lut) and galangin (Gal), which have features belonging to both the (i) and (ii) categories defined in the Introduction, as well as quercetin (Que), which exhibits the characteristics of both (i) and (ii) categories and has therefore the highest degree of variability in terms of complexation with metals. The initial structures of those flavonoids were based on the flavone structure.^{11,24} Substitution of the OH at positions 5, 7, 3', 4', and 3 yields the quercetin molecule (shown in Figure 1), at positions 5, 7, 3', and 4' yields the luteolin molecule, and at positions 3, 5, and 7 gives the galangin molecule. For the geometry optimization, the structure is considered fully relaxed when the magnitude of forces on the atoms is smaller than 0.04 eV/Å. As representative examples, the calculated bond length of Que between C4=O4 is 1.279 Å (1.267, 1.285, 1.262), between C4–C3 it is 1.445 Å (1.440, 1.449, 1.440), and between C2–C1' it is 1.456 Å (1.479, 1.452, 1.462), all in good agreement with the corresponding experimental³¹ and two other values obtained with the generalized gradient approximation,³⁴ which are given in parentheses in that order, respectively. For all cases, molecules (Cu complexes) were treated in a supercell scheme allowing enough empty space between molecules to make intermolecular interactions negligible. In particular, we used an empty space equal to half of the maximum molecular length. The calculated values are well converged in this respect, as evidenced by the fact that if we double or triple the supercell size the results concerning the total energy and structural relaxations are the same.

For the optical absorption calculations within TDDFT in the linear response formulation,³² 6107 steps in time were used to propagate the wave functions with a time step of 3.4×10^{-3} fs, which gives an energy resolution of 0.1 eV. The perturbing external electric field is 0.1 V/Å. This computational scheme gives optical absorption spectra that are in good agreement with experiment for a range of biologically relevant molecules such as DNA bases.³³

III. Structural Properties

We evaluate the ability of flavonoids to bond to Cu ions by calculating the binding energy for complexes at different chelation sites (CS). After structural optimization of the Cu–Que and Cu–Gal complexes, we find that the preferred CS of the Cu ion involves the detachment of a H atom from the OH group at the 3 site and formation of covalent bonds with the O atoms at sites 3 and 4. For the quercetin and the luteolin cases, another favorable CS site exists at the 3'–4' *ortho*-dihydroxyl groups of ring B. We calculate the binding energy of the flavonoid structures involving the removal of H atoms from OH units to which the Cu atom is bonded, by taking into account the relevant chemical potential. To this end, we choose two reservoirs that approximately correspond to the limiting cases of acidic (H₂ molecules) and basic (H₂O molecules) solutions (for details of this approach, see ref 24).

For the 1:1 complex, we consider the CS close to the oxo-group, denoted as 3–4 and 4–5, as well as the CS at 3'–4' that involves the removal of one H atom, denoted as ($3_{H'}-4'$), with the subscript H indicating the site from which the H atom is not removed, or two H atoms, denoted as ($3'-4'$). For the 1:2 complex, we assume three highly symmetric structures: (a) the two molecules are coplanar and there is a reflection symmetry plane perpendicular to the plane of the molecule and passing through the position of the Cu atom, (b) two coplanar

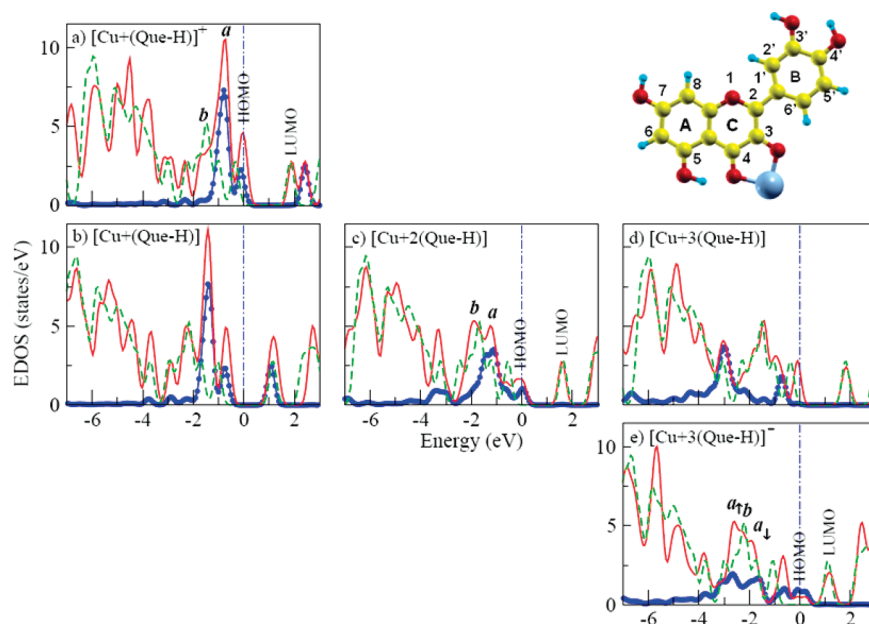


Figure 1. EDOS of the Cu–quercetin complexes (red solid line) for (a) the 1:1 positively charged complex, (b) the 1:1 neutral complex, (c) the neutral 1:2 complex, (d) the neutral 1:3 complex, and (e) the negatively charged 1:3 complex. a_1 and a_2 correspond to spin majority and spin minority decomposition of the a -state. The dashed green line corresponds to EDOS of the single quercetin molecule, the blue line with dots refers to the partial EDOS of the Cu atom within the complex, and the vertical dashed-dotted line denotes the Fermi level. The geometry of a single Que complex is represented by gray, red, yellow, and blue spheres for the Cu, O, C, and H atoms, respectively, at the upper right corner.

molecules with inversion symmetry in the plane with respect to the Cu atom position, (c) the planes of the two molecules bound by a single Cu are orthogonal to each other, with the Cu atom adopting an octahedral-like structure, and (d) the trigonal bipyramid structure. Depending on the CS of Cu and the relative position of the two molecules, we define the structures as (3–4;3–4)^a, (4–5;4–5)^a, and (3–4;4–5)^a for the (a) structure defined above, (3–4;3–4)^b, (4–5;4–5)^b, and (3–4;4–5)^b for the (b) structure, the (3–4;3–4)^c for the (c) structure, and the (3–4;3–4)^d for the (d) structure. As far as the 1:3 complex is concerned, the three molecules are mutually perpendicular in all four combinations of 3–4 and 4–5 CS (3–4;3–4;3–4), (3–4;3–4;4–5), (3–4;4–5;4–5), and (4–5;4–5;4–5), with the Cu atom assuming a fully octahedral coordination. In Table 1, we present the complex binding energies E_b and E_b' depending on the reservoir choice, which are calculated as:

$$E_b = E_{\text{total}} - n_{\text{Cu}}E_{\text{Cu}} - n_{\text{Que}}E_{\text{Que}} + n_{\text{H}}E_{\text{H}} + n_{\text{H}}\frac{1}{2}E_{\text{H}_2} \quad (1)$$

$$E_b' = E_{\text{total}} - n_{\text{Cu}}E_{\text{Cu}} - n_{\text{Que}}E_{\text{Que}} + n_{\text{H}}E_{\text{H}} + n_{\text{H}}\frac{1}{2}(E_{\text{H}_2\text{O}} - E_{\text{H}} - E_{\text{OH}}) \quad (2)$$

where E_{total} is the total energy of the complex, E_X and n_X are the energy and number of species X involved in the complexation reaction ($X = \text{Cu}, \text{Que}, \text{H}, \text{OH}, \text{and } \text{H}_2\text{O}$), and E_{H_2} , $E_{\text{H}_2\text{O}}$, and E_{OH} are the binding energy of the corresponding molecules.

We find that in all cases the preferred CS is close to the 4 carbonyl group. In particular for the 1:1 complex, the CS 3–4 is energetically favored for both reservoirs while due to steric repulsion the next energetically favored position 4–5 of quercetin and galangin is unable to chelate additional Cu. Moreover, for quercetin and luteolin a second Cu atom can be chelated at the 3'–4' site with one H removal. For the 1:2 complex, we focus on the oxo-group chelation sites and we confirm the (3–4;3–4) as the energetically favored combination of sites consistent with the preferred CS site in the 1:1 complex.

More specifically, the 1:2 complex prefers the orthogonal arrangement of the molecules (3–4;3–4)^c, followed by the (3–4;3–4)^a and (3–4;3–4)^b structures. The trigonal bipyramid (3–4;3–4)^d geometry for the 1:2 complex with coordination number 4 is found to be energetically unfavored compared to the other 1:2 structures. Finally, the 1:3 complex octahedral structure also prefers the 3–4 CS for the three molecules, referred (3–4;3–4;3–4) position compared to the other combinations of sites. These results show that Cu ions exhibit the same preference for CS as Fe ions do.²⁴

The choice of H_2 and H_2O molecules in eqs 1 and 2 as molecular reservoirs rather than as explicit peripheral ligands is not enough to simulate an acidic and a basic solution, respectively. Nevertheless, it provides information about the energetically favored chelation sites and the corresponding favored stoichiometries in a thermodynamically consistent framework, and therefore it can be regarded as a good approximation for these limiting solutions. As seen from Table 1, for all stoichiometries and using either eq 1 or eq 2, the CS 3–4 is energetically favored for all Cu complexes. In addition, Cu shows the tendency to fulfill its coordination number as the pH increases and indeed the binding energy of the 1:1 complex in the “acidic”-like solution is energetically favored over the “basic”-like solution (Table 1), in agreement with the experimental findings.⁹

To understand in detail the influence of OH or H_2O ligands in the structural and optical properties of our complexes, we performed TDDFT calculations for selected cases. For the Cu–Que complexes solvated by OH groups or H_2O molecules, the Cu–O bond length variations are dominated by the chemical nature of the Que, OH, and H_2O groups, which overwhelm the Jahn–Teller distortions that can occur in these complexes.^{35,36} For instance, in Table 2, the average Cu–O bond lengths for Que–Cu, Cu–OH, and Cu– H_2O bonding are 1.99, 1.79, and 2.16 Å, respectively, in the case of 2Que–Cu (planar) solvated by OH or H_2O groups, which agrees with the general chemical trends.

TABLE 2: Average Cu–O Bond Length of Selective Cu–Que Complexes Solvated by OH Groups or H₂O Molecules^a

complex	solvate	<i>N</i>	<i>d</i> (Å)	<i>d</i> _{OH} (Å)	<i>d</i> _{H₂O} (Å)
Cu–Que (3–4)		2	1.97		
	2 OH	4	1.99	1.86	
	2 H ₂ O	4	1.97		2.00
	4 OH	6	1.99	1.83	
Cu–2Que (3–4;3–4) ^a		4	1.96		
	2 OH	6	1.99	1.79	
	2 H ₂ O	6	1.99		2.16
Cu–2Que (3–4;3–4) ^d		4	1.92		
	1 OH	5	1.96	1.82	
	1 H ₂ O	5	1.93		2.01

^a *d* is the Cu–Que bond, *d*_{OH} is the Cu–OH bond, and *d*_{H₂O} is the Cu–H₂O bond. The number of Cu–O bonds (*N*) is also given in each case.

IV. Electronic and Optical Properties

Of all the cases we studied involving three different flavonoid molecules, we will analyze in detail the electronic and optical properties of quercetin, which has the largest number of OH groups and thus has the highest degree of variability in terms of complexation with metals. We discuss first the electronic density of states (EDOS), which provides an overall picture of the relevant electronic states, we present next the results of TDDFT calculations for the optical absorption properties, which can be directly compared to experimental results, and finally we provide a detailed discussion of the wave functions of states around the Fermi level, which are useful in interpreting the nature of the optical transitions.

We calculated the EDOS for the lowest-energy configurations of the Cu–Que complexes shown in Table 1. In Figure 1, we present the EDOS of the complexes we considered in various charge states. To facilitate comparisons, we arranged the results in a table format with each column containing results for the same complex but in different charge states and each row corresponding to the same charge state, but for different complexes. Not all entries of this table of figures are present, because we focused on the most likely complex states, assuming that the Cu ion has charge +2 in solution (Cu²⁺) and that each Que molecule can be easily deprotonated at one OH site where Cu binds, giving it a charge of –1. With these assumptions, the most likely state for the 1:1 ratio is a positively charged, for the 1:2 ratio a neutral, and for the 1:3 ratio a negatively charged complex. For each complex, we also included the neutral case as a reference state. Thus, Figure 1 includes the 1:1 positively charged (first row, Figure 1a), 1:1, 1:2, and 1:3 neutral (middle row, Figure 1b,c,d), and 1:3 negatively charged (third row, Figure 1e) complexes. In each case, we also include the EDOS of the pure quercetin molecule and the partial EDOS for the Cu ion within the complex.

In comparison with the pure Que molecule, the highest occupied molecular orbital (HOMO) of the positively charged 1:1 Cu complex is located at the Fermi level, as shown in Figure 1a. In addition, the corresponding band gap decreases from 2.2 to 1.9 eV, in agreement with the Fe–Que case.²⁴ A similar trend is encountered in the 1:2 and 1:3 complexes, as depicted in Figure 1c–e. The HOMO state consists of Cu, C, and O orbitals for these Cu complexes, except for the neutral 1:3 complex, which has no contribution from the Cu orbital. The lowest unoccupied molecular orbital (LUMO) is dominated by C *p*-orbitals, except for the 1:1 neutral complex.

The Cu ion induces a sharp peak at –0.72 eV for the 1:1 complex in Figure 1a (labeled and referred to in the following

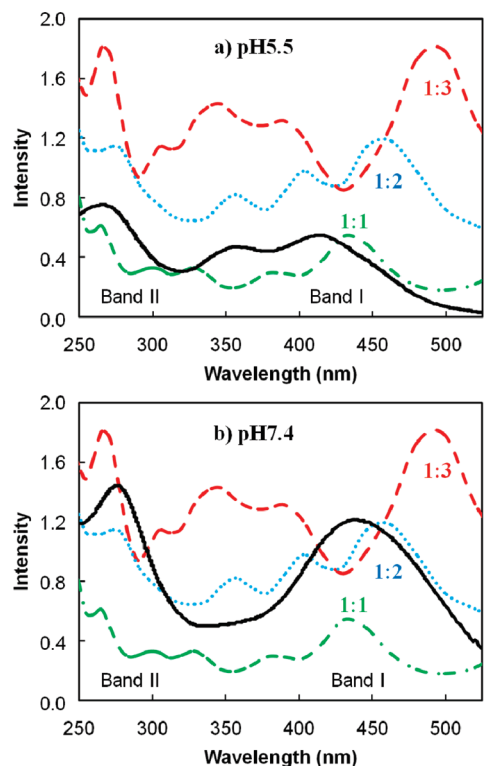


Figure 2. UV–vis experimental spectra (solid line) for (a) pH 5.5 and (b) pH 7.4 together with the calculated curves for Cu–Que complexes with stoichiometries 1:1 (dashed-dotted green line), 1:2 (dotted blue line), and 1:3 (dashed red line).

as “*a*-state”). The corresponding *a*-states of the 1:2 and 1:3 complexes, however, are broader and less prominent, as shown in Figure 1c,e, due to the strong interaction of the Cu and Que molecule. In addition, the peak around –2.0 eV (labeled “*b*-state”), which is almost unoccupied in the 1:1 complex, is gradually occupied mostly by C-derived states in going from 1:2 to 1:3 complexes (Figure 1c–e), which suggests that the presence of Cu induces coupling between states in the two or the three quercetins, respectively. In the 1:3 complex, the *b*-state is characterized by the contributions of C and O and the *a*-state splits in two major peaks (*a*₁ and *a*₂) that correspond to spin majority and spin minority states. The strong coupling of the Que molecules gradually dominates the EDOS of the complexes below –4.0 eV.

Concerning the optical properties of these complexes, electrospray ionization mass spectrometry data^{8,9} showed that for pH ≤ 5.5 the Cu–quercetin complexes have stoichiometries 1:1 and 1:2, while the typical band I of quercetin (peak at 372 nm) undergoes a large bathochromic shift to 412 nm, decreasing in absorbance, with a small shoulder around 360 nm. Moreover, band II (pure quercetin peak at 256 nm) demonstrates a smaller bathochromic shift (with the complex peak at 270 nm) and decreases in absorbance. Interestingly, at pH 7.4 bands I and II are experimentally found to be shifted to 436 and 280 nm, respectively, and it has been suggested that this is due to the formation of the 1:3 complex.⁹

To elucidate the complexation mechanism of flavonoids with the Cu ion, as this is reflected in the optical absorption spectra, we calculate the optical properties of the Cu complexes with TDDFT. Our results are presented in Figure 2. For the 1:1 complex, there are two absorbance bands located in the visible region. The wavelength of band I is close to the first peak at 412 nm, and band II is located at 270 nm, which are in good

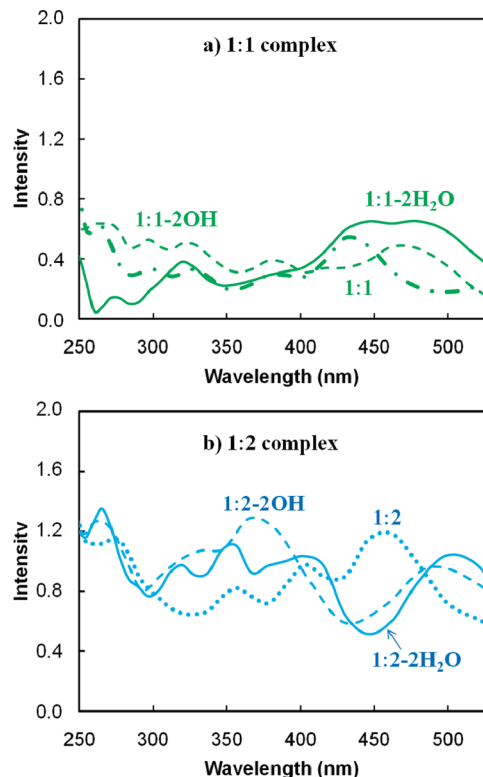


Figure 3. UV-vis spectra of (a) 1:1 complex (dashed-dotted green line) and (b) 1:2 complex (dotted blue line) solvated by OH (dashed line) or H₂O (solid line) ligands.

agreement with the UV-vis spectra at pH 5.5 (Figure 2a). For the 1:2 complex (Figure 2b), bands I and II have been red-shifted slightly, and the small peaks between the two bands are more obvious, in contrast with the 1:1 complex. The first absorption peak of the 1:3 complex moves to 490 nm, and the second one is still around 270 nm, which are in good agreement with the experimental values at pH 7.4. With the increase of concentration of quercetin molecules, the position and intensity of the first absorption peak are gradually red-shifted and enhanced.

When the bare Que-Cu complexes are solvated by several OH and H₂O molecules, the coordination number of the Cu ion is increased to 4–6, as shown in Figure 3a,b. The major features in the optical spectrum of these solvated complexes are determined by the coordination number rather than the Que-Cu ratio. For instance, the position of the first peak is largely red-shifted after solvation, from 430 to 462 nm in the case of the Cu-Que 1:1 complex, and from 446 to 487–500 nm in the case of the Cu-Que 1:2 complex. Consequently, the spectra for solvated 1:1 and 1:2 complexes greatly resemble those for bare 1:2 and 1:3 complexes. The big feature around 310–380 nm shown in the spectra for the solvated 1:2 complex and the bare 1:3 complex also confirms this point, since in both cases the coordination number of Cu ion is 6. Therefore, compared to the experimental spectrum measured at pH = 7.4, neither of them represent a good structural candidate for the optimal complex under this condition. Similarly, the solvated 1:1 complexes show peaks around 300–320 nm, which are absent in the measured spectrum at pH = 7.4, though they all exhibit a main peak around 450 nm, making these complexes unsuitable candidates. The calculated spectra for hydrated trigonal bipyramidal structures (not shown here) also contain features that are significantly different from the measured ones. In conclusion, the bare Cu-Que = 1:2 complex with a Cu coordination number

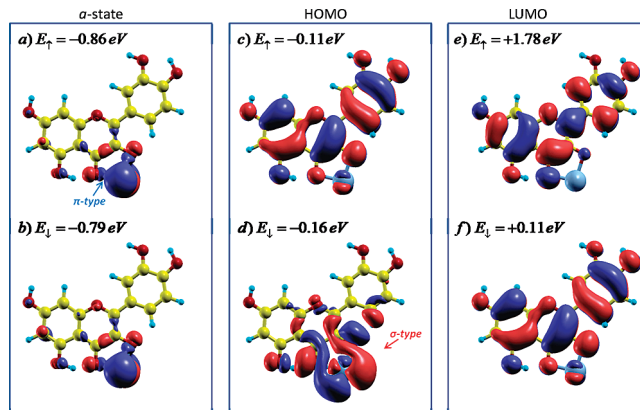


Figure 4. Wave functions of the Cu-Que complex: (a, b) *a*-state, (c, d) HOMO state, and (e, f) LUMO state. In each case, the upper and lower panels show the spin majority and minority states, respectively. Blue (red) isosurfaces correspond to positive (negative) values. The states that contribute to σ and π bonding between the metal atom and the molecule are indicated.

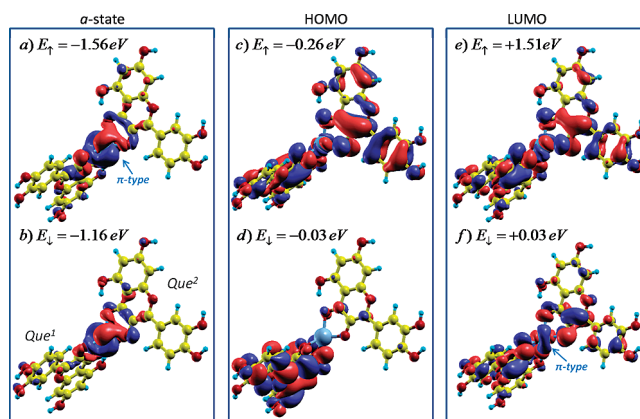


Figure 5. Wave functions of the Cu-2Que complex: (a, b) *a*-state, (c, d) HOMO state, and (e, f) LUMO state. Notation is the same as in Figure 4.

of 4 represents the best structural candidate among all structures studied above for the complex measured in experiment at pH = 7.4.

For all complexes, the HOMO-LUMO transitions as well as the *a*-state and *b*-state transitions are mainly responsible for band I, whereas transitions from lower energy states result in absorbance corresponding to band II. In particular, the Cu-dominated *a*-state is mainly responsible for the absorbance of band I, whereas the *b*-state that is energetically responsible for the experimental peak around 360 nm at both pH 5.5 and 7.4 comes from the contribution of the Que molecules. Finally, band II is due to transitions from energies below -3.0 eV that are mainly occupied by states related to the Que molecules of the complex.

The wave functions around the Fermi level, corresponding to the different complexes, are shown in Figures 4–6. For the 1:1 complex, the *a*-states for both spin configurations (Figure 4a,b) are dominated by the Cu d_{z^2} orbitals, which form π bonds with the p_x , p_y orbitals of the neighboring O atoms. The majority spin state of the HOMO (Figure 4c) primarily comprises a linear combination of p_z orbitals of the C and O atoms with mainly π bonding character. The minority spin state, shown in Figure 4d, however, is based on the overlap of the $3d_{x^2-y^2}$ and $3d_{xy}$ of Cu, and $2p_x$, $2p_y$ of the C and O atoms. It is interesting that in the minority spin state the σ -type bonding character is dominant. Similarly, both spin states of the LUMO, shown in Figure 4e,f, are located on the entire Que molecule. The majority spin comprises

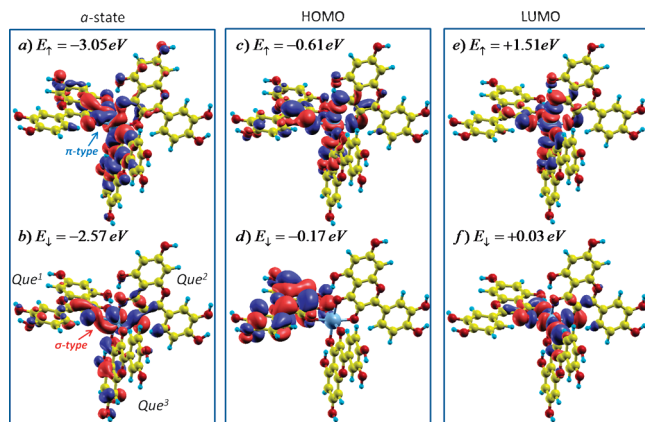


Figure 6. Wave functions of the Cu–3Que complex: (a, b) a -state, (c, d) HOMO state, and (e, f) LUMO state. Notation is the same as in Figure 4.

mainly antibonding combinations. Therefore, the optical absorption band has $\pi \rightarrow \pi^*$ and $\sigma \rightarrow \pi^*$ character. The minority spin state corresponds to the half-unoccupied state closest to the Fermi level, whereas the other half-occupied state corresponds to the HOMO state in Figure 4a, explaining the similar orbital distribution.

In Figures 5 and 6, we present selective wave functions of the 1:2 and 1:3 complexes. The a -state is localized on the Cu ion, bonded to the Que¹ and Que² molecules with π -type bonds in the 1:2 complex, whereas the HOMO spin minority state of the 1:3 complex exhibits σ -type bonding character. The HOMO spin minority state of both complexes is confined to one of the two Que molecules. The other 1:2 complex wave functions are spread over the entire complex, whereas the Cu d orbitals show π -type bonding or antibonding character with the neighboring O orbitals. As far as the 1:3 complex is concerned, the HOMO spin majority and the LUMO states are characterized by strong localization in the center of the complex that involves the Cu atom and its first neighbor O orbitals and exhibit π -type antibonding character. Consequently, the first absorption band of the 1:2 and 1:3 complexes has $\pi \rightarrow \pi^*$ character, whereas the σ -bonding features of the a -states suggest the existence of $\sigma \rightarrow \pi^*$ character in the lower wavelength optical absorption band of the 1:3 complex.

V. Conclusions

Our DFT- and TDDFT-based investigation of the structural, electronic, and optical properties of Cu–quercetin complexes shows that for all metal-to-flavonoid molar ratios (1:1, 1:2, and 1:3) the energetically favored chelation site of Cu²⁺ is the 4-oxo group and in particular the 3–4 site, whenever there is an OH moiety at position 3, followed by the 3′–4′ dihydroxyl structure in ring B, in agreement with calculations on related Fe–flavonoid complexes.²⁴ In the Cu–Que complexes, the Cu²⁺, inducing a new HOMO state, reduces the band gap of the pure quercetin molecule, which explains the red shift of the first absorption band upon complexation observed in UV–vis spectra. The HOMO state incorporates the contribution of Cu, C, and O orbitals, whereas the LUMO is dominated by the C p_z orbitals. Although the a -state of 1:1 and 1:2 complex is localized on the Cu ion and therefore is a single occupied molecular orbital (SOMO), it is different from the corresponding SOMO states in Fe–flavonoid complexes that are located between the HOMO and LUMO states.²⁴ In the EDOS of the Cu–Que complexes, new states appear and are enhanced by the increasing molar ratio of the flavonoid, playing an important

role in the optical response. The HOMO state of the Cu–flavonoid complexes is characterized by π -type bonding between the Cu and the Que molecules, whereas the spin minority HOMO and a -state of the 1:1 and 1:3 complexes exhibit σ -type bonding, respectively. The 1:1 complex has an optical absorption spectrum very similar to the experimental absorption at pH 5.5, whereas the spectrum of the 1:2 complex follows closely the spectra observed in experiments at pH 7.4.

Acknowledgment. We thank D. Galaris for fruitful discussions.

References and Notes

- (1) Havsteen, B. H. *Pharmacol. Ther.* **2002**, *96*, 67.
- (2) Rice-Evans, C.; Miler, N. J.; Pananga, G. *Free Radical Biol. Med.* **1996**, *20*, 956.
- (3) Ishige, K.; Shubert, D.; Sagara, Y. *Free Radical Biol. Med.* **2001**, *30*, 433.
- (4) Suzuki, Y.; Forman, H.; Svanian, A. *Free Radical Biol. Med.* **1997**, *22*, 269.
- (5) Di Carlo, G.; Mascolo, N.; Izzo, A. A.; Capasso, F. *Life Sci.* **1999**, *65*, 337.
- (6) McCord, J. M.; Day, E. D., Jr. *FEBS Lett.* **1978**, *86*, 139.
- (7) Halliwell, B. *FEBS Lett.* **1978**, *92*, 321.
- (8) Fernandez, M. T.; Mira, M. L.; Florencio, M. H.; Jennings, K. R. *J. Inorg. Biochem.* **2002**, *92*, 105.
- (9) Mira, L.; Fernandez, M. T.; Santos, M.; Rocha, R.; Florenchio, M. H.; Jennings, K. R. *Free Radical Res.* **2002**, *36*, 1199.
- (10) De Souza, R. F. V.; Sussuchi, E. M.; De Giovanni, W. F. *Synth. React. Inorg. Met.-Org. Chem.* **2003**, *33*, 1125.
- (11) Melidou, M.; Riganakos, K.; Galaris, D. *Free Radical Biol. Med.* **2005**, *39*, 0000.
- (12) Aruoma, O. *Free Radical Biol. Med.* **1996**, *20*, 675.
- (13) Hynes, M. J.; O’Coineannainn, M. *J. Inorg. Biochem.* **2004**, *98*, 1457.
- (14) Ozgova, S.; Hermanek, J.; Gut, I. *Biochem. Pharmacol.* **2003**, *66*, 1127.
- (15) Khokhar, S.; Apenten, R. K. O. *Food Chem.* **2003**, *81*, 133.
- (16) De Souza, R. F. V.; De Giovanni, W. F. *Redox Rep.* **2004**, *9*, 97.
- (17) De Souza, R. F. V.; De Giovanni, W. F. *Spectrochim. Acta, Part A* **2005**, *61*, 1985.
- (18) Deng, H.; van Berkel, G. J. *J. Mass Spectrom.* **1998**, *33*, 1080.
- (19) Kuo, S.-M.; Leavitt, P. S.; Lin, C.-P. *Biol. Trace Elem. Res.* **1998**, *62*, 135.
- (20) Le Nest, G.; Caille, O.; Woudstra, M.; Roche, S.; Burlat, B.; Belle, V.; Guigliarelli, B.; Lexa, D. *Inorg. Chim. Acta* **2004**, *357*, 2027.
- (21) Pusz, J.; Nitka, B.; Zielinska, A.; Wawer, I. *Microchem. J.* **2000**, *65*, 245.
- (22) Roshal, A. D.; Grigorovich, A. V.; Doroshenko, A. O.; Privovarenko, V. G.; Demchenko, A. P. *J. Photochem. Photobiol., A* **1999**, *127*, 89.
- (23) Kopacz, M.; Kopacz, S.; Skuba, E.; Russian, J. *Gen. Chem.* **2004**, *74*, 957.
- (24) Ren, J.; Meng, S.; Lekka, Ch. E.; Kaxiras, E. *J. Phys. Chem. B* **2008**, *112*, 1845.
- (25) Sanchez-Portal, D.; Ordejon, P.; Artacho, E.; Soler, J. M. *Int. J. Quantum Chem.* **1997**, *65*, 453.
- (26) Artacho, E.; Sanchez-Portal, D.; Ordejon, P.; Garcia, A.; Soler, J. M. *Phys. Status Solidi B* **1999**, *215*, 809.
- (27) Soler, J.; Artacho, E.; Gale, J. D.; Garcia, A.; Junquera, J.; Ordejon, P.; Sanchez-Portal, D. *J. Phys.: Condens. Matter* **2002**, *14*, 2745.
- (28) Troullier, N.; Martin, J. L. *Phys. Rev. B* **1991**, *43*, 1993.
- (29) Kleinman, L.; Bylander, D. M. *Phys. Rev. Lett.* **1982**, *48*, 1425.
- (30) Junquera, J.; Paz, O.; Sanchez-Portal, D.; Artacho, E. *Phys. Rev. B* **2001**, *64*, 235111.
- (31) Rossi, M.; Rickles, L. F.; Halpin, W. A. *Bioorg. Chem.* **1986**, *14*, 55.
- (32) Tsolakidis, A.; Sanchez-Portal, D.; Martin, R. M. *Phys. Rev. B* **2002**, *66*, 235416.
- (33) Tsolakidis, A.; Kaxiras, E. *J. Phys. Chem. A* **2005**, *109*, 2373.
- (34) Mendoza-Wilson, A. M.; Glossman-Mitnik, D. *J. Mol. Struct.: THEOCHEM* **2004**, *681*, 71.
- (35) Stevenson, C. D.; Kim, Y. S. *J. Am. Chem. Soc.* **2000**, *122*, 3211.
- (36) Bearpark, M. J.; Blancafort, L.; Robb, M. A. *Mol. Phys.* **2002**, *100*, 1735.